RSC Advances

ROYAL SOCIETY OF CHEMISTRY

www.rsc.org/advances

Biomaterials Functionalized Graphene Oxides with Tunable Work Function for High Sensitive Organic Photodetectors

Zhimei Hu,[a] Chi Li,[b] Riming Nie,[a] Yan−Qing Li,[b] Jian−Xin Tang,[*,b] and Xianyu Deng[*,a]

[a]Research Center for Advanced Functional Materials and Devices, Shenzhen Key Laboratory of Advanced Materials, School of Materials Science and Engineering, Shenzhen Graduate School, Harbin Institute of Technology, Shenzhen 518055, PR China.

[b]Jiangsu Key Laboratory for Carbon-Based Functional Materials and Devices, Institute of Functional Nano & Soft Materials (FUNSOM), Soochow University, Suzhou 215123, PR China.

* Address correspondence to jxtang@suda.edu.cn, xydeng@hitsz.edu.cn

ABSTRACT

Graphene acts as an ideal material for transparent conductive electrode in optoelectronic devices attributed to its excellent electrical conductivity, optical transparency, and mechanical properties. Graphene oxide (GO) in the form of colloidal suspension is considered to be more commonly useful because of its low cost and high volume production. However, controlling the work function of graphene and GO as transparent electrodes in optoelectronic devices is still a challenging task,

since it is important to match the energy level of the active materials. In this study, GO sheets functionalized with amino acids were fabricated via a mild and environmentally friendly approach. The work functions of the novel amino acids functionalized graphenes and their compounds with poly(3, 4−ethylenedioxythiophene) polystyrene sulfonate (PEDOT: PSS) were tuned over a wide range, which matched well with the energy of various semiconductors. Organic photodetectors with the functionalized GO exhibited the highest normalized detectivity of 5.7×10^{12} Jones at −0.1 V. The results indicated that the synthesized solution−processable GO exhibits a promising potential as transparent electrodes for various photoelectric devices.

Keywords: Graphene, Biomolecules, Amino acids, Transparent conductive electrodes, Organic electronics

Introduction

Graphene oxide (GO), a two dimensional nanostructure material, exhibits a promising potential in the applications of various optoelectronic devices[1–4]. In general, GO is obtained by the chemical oxidation of graphite. Modified Hummers method[5] is a classical technique to prepare GO, wherein large-scale production of GO is easily possible. GO possesses the excellent feature of solution-processing with water/alcohol attributed to its significant amounts of oxygen−carrying groups such as carboxyl, hydroxyl, and epoxy[6]. These reactive oxygen groups make GO hydrophilic; thus it disperses well in water/alcohol solvents, which allows its uniform deposition onto substrate via some simple methods such as solution processes of ink−jet printing and spin coating[7]. GO in the form of colloidal suspension is not only scalable for high volume production at low costs, but also compatible with emerging technologies based on flexible substrates.

Graphene and GO can be used as new generation potential candidates for transparent conductive electrodes. Till date, indium tin oxide (ITO) is the most widely used transparent window electrode in numerous photoelectric devices. However, ITO seems unsustainable because of the scarcity of indium in the earth. Thus, alternatives to ITO are urgently required. Graphene is a material with high light transmittance, and it exhibits ultra−high conductivity because its band gap is close to zero, thus graphene and its derivate GO are considered as the most promising next generation candidates for the transparent conducting electrode of optoelectronic devices[8–14]. In order to obtain significantly high device performance, it is extremely important to match the

work function of an electrode to the energy levels of an active layer in devices for the efficient transfer of hole or electron between the electrode and the active layer. However, the work function of graphene (4.7 eV) and GO (5.3 eV) does not match well with the molecular energy levels of most active materials. Therefore, controlling the work functions of graphene or GO is essential for its applications in photoelectric devices.

Biomolecules are selected as preferred functional groups grafted on various types of materials to realize novel functions because they have some inherent advantages such as low cost, environmentally friendly, and wide existence in the nature. GO can be readily functionalized using appropriate biomolecules through chemical reactions due to the presence of abundant active oxygen-carrying functional groups in GO. Functionalized GO derivatives have been proved as promising candidates exhibiting potential applications in some important fields such as drug-delivery vehicles[15, 16], biosensors, and catalysis[17, 18]. Biomolecules such as amino acids and peptides with large molecule dipoles and excellent charge transport properties may act as favorable medium in the use of electronic devices. However, applications of biomolecules functionalized graphene or GO in the electronic devices have rarely been investigated.

In this study, GO was functionalized with a series of amino acids with the objective of controlling its work function. The synthesized GO derivatives were characterized by Fourier transform infrared spectroscopy (FT−IR), X−ray diffraction (XRD), scanning electron microscopy (SEM), atomic force microscopy (AFM), transmission electron microscopy (TEM), and X−ray photoelectron spectroscopy

(XPS). The results indicated that amino acids were covalently grafted to the GO by forming amide bonds. Ultraviolet photoelectron spectroscopy (UPS) was used to determine the work function. The work function of GO could be controlled over a wide range from 5.3 to 4.0 eV corresponding to non-functionalized and amino acids functionalized GO. Further, the as−prepared graphene compounds were blended with PEDOT: PSS. The work function of the above mentioned hybrid materials could also be controlled by GO with different amino acids.

Results and discussions

GO was prepared by the modified Hummers method[5]. The as−prepared GO and sodium chloroacetate were dispersed in alkaline solution. The contents were ultrasonicated for 4 h, which resulted in the conversion of the hydroxyl groups on the edge of the original GO into carboxyl groups. Thus, carboxylated GO was obtained and was denoted as GO–COOH. First, the carboxylic groups on the GO–COOH were required to be activated prior to their functionalization with amino acids. In general, the carboxyl groups present on the edge of GO are activated using $SOCl_2$[19–21], EDC, and DCC[22]. In this study, different types of amino acids were used in the synthesis of amino acid functionalized GO. The process of synthesis is illustrated in Scheme 1. First, GO is treated with sodium chloroacetate and then activated by $SOCl_2$ at 65 °C for 24 h, and the product is denoted as GOCl. Subsequently, GOCl is reacted with amino acids in a solution at 90 °C for 24 h. The so−obtained amino acid functionalized GO is denoted as GO−AA.

The size and morphology of GO−AAs were characterized by SEM, TEM, and AFM. Figure 1a shows the SEM images of GO functionalized with cysteine (GO–Cys). Figure 1a shows the morphology of GO–Cys, revealing the presence of wrinkled, folded, and ultra−thin silk−like lamellas. SEM images of graphite oxide and GO are shown in SI Figure S1. Figure 1b displays the TEM images of GO–Cys. Apparently, GO–Cys sheets are thin, light, and transparent with some pleats on the surface, at low magnification. However, at high magnification, GO–Cys sheets are clearly observed to be stacked. AFM is a common tool to measure the thickness of graphene. In general, the thickness of a monolayer graphene sheet is about 1.2 nm[23] and the number of graphene layers can be deduced from the obtained thickness. Figure 1c shows the AFM images and height profiles of GO–Cys. The thickness of GO–Cys sheets was about 2 nm; therefore, the results indicated that the measured samples had one or two layers of sheets.

The as−synthesized GO was characterized by both FT−IR spectroscopy and XPS in order to confirm the formation of the composite. Figure 2a shows the FT−IR spectra of GO, GO–COOH, GO–Ala, GO–Cys, and GO–Ser. The spectrum of GO exhibits the peaks corresponding to C=O and C=C stretching vibrations at 1722 and 1630 cm^{-1}, respectively. The peaks at 3400 and 1380 cm^{-1} are attributed to absorbed water. The peaks at 1220 and 1050 cm^{-1} are corresponding to the stretching vibrations of C–O–C and C–O, respectively. The spectrum of GO–COOH shows the peaks at 1640 and 1080 cm^{-1}, corresponding to carboxyl and epoxy groups present on GO–COOH, respectively. Following the functionalization of the carboxylated GO by

amino acids, the new peaks at 1635 and 1565 cm^{-1} are attributed to amide (I) and amide (II) vibrations[24], respectively. Besides, the appearance of peaks at 2929 and 2853 cm^{-1} are attributed to the stretching vibrations of CH_2 which exists in the structure of amino acid molecules. The FI−IR spectra of other four types of amino acids grafted on GO are shown in SI Figure S2. The above mentioned results demonstrated that the amino acids were successfully grafted onto the GO sheets by forming amide bonds. Moreover, XPS results were analyzed in this study in order to further explore the structure of the composites. Figure 2b shows the C1s spectrum of GO–Cys exhibiting four peaks, which are assigned to C=C (284.5 eV), C–O (285.8 eV), C–N (286.6 eV), and C=C/C–C (288.6 eV). Figure 2b (left) presents the N 1s spectra of GO–Ser and GO–Cys at 400 eV, which is a powerful evidence to determine the amino acids bonded on top of GO sheets through amidation.

UPS was performed to characterize the work function of GO and GO−AA compounds. Figure 3a shows the results of UPS of GO and GO−AAs, indicating that the work function of non−functionalized GO prepared by modified Hummers method, is about 5.3 eV. However, the work function of GO−AAs decreases to 4.0–4.5 eV. For thin-film optoelectronic devices, the device performances are critically dependent on the relative alignment of the highest occupied molecular orbital (HOMO) and the lowest unoccupied molecular orbital (LUMO) levels of the active material with the work function of the electrodes in contact. Graphene and its derivate GO are potential candidates for electrodes, with applications in many different types of optoelectronic devices with the compatibility of printable, large scale, and flexible fabrication, such

as organic electronic devices and perovskite thin-film electronic devices, due to their good light transmission property and conductivity. A suitable energy level match between an electrode and a semiconductor should make the contact as ohmic as possible. This requires the work function of the electron selective electrode (cathode) close to or lower than the LUMO of the semiconductor and the work function of the hole selective electrode (anode) close to or higher than the HOMO of the semiconductor. The work function of the GO in this study was controlled over a wide range of 5.3 to 4.0 eV which could match the HOMO levels of the commonly used organic semiconductors, such as MEH−PPV (5.3 eV) and P3HT (5.2 eV), as well as the LUMO levels of some organic and inorganic semiconductors, such as PCBM (4.0 eV), TiO2 (4.2 eV), and ZnO (4.4 eV) [25].

Figure 3 indicates the effect of the structure of the amino acids on the work function of GO. Amino acids are classified into several types based on the side chain group R in the structure. Based on the electric property, the side chain R of amino acids can be classified into positive and negative groups. Interestingly, the work function of GO−AA is conformed to certain rules. Obviously, the GO−AA with positive charged side groups (Arg 4.5 eV and Lys 4.45 eV) shows less change in the work function compared to the GO−AA with negative charged side groups. The GO−AA with electron−rich thiol group (Cys 4.1 eV) exhibits the largest change in the work function. According to the literature reports, a positive charged amino group (–NH_2–) was demonstrated to have a positive effect on the reduction of the work function of ITO surface modified with the amino acids and peptides[26–28]. During the

modification of the ITO surface, positive amino group produced large dipoles along the surface, leading to a significant reduction in the surface work function. However, herein the reduction in the work function was attributed to different mechanistic approach. As well known, the effect of surface dipole on the work function change is intensively depended on the surface dipole density. Therefore, it requires a high density of amino acids on the surface of GO if the work function change is caused by the effect of surface dipole. However, in SI Figures S3 and S4 which show the XPS results, it reveals the existence of a very low density of amino acid on top of the GO. This indicates that the surface dipoles are not the main factor on the work function change. We attributed the change in work function of GO mainly to the change in electron distribution over the entire GO molecule, which was caused by the additional amino acid molecules.

When the amino acids are grafted on GO, concomitant occurrence of reduction reaction of GO is also possible, which may lead to a change in the work function. To investigate the possible effects of the reduction reaction on the change in the work function, we calculated C: O ratios of GO and GO−AA, which are listed in Table 1. The values listed in Table 1 indicate that the ratios of C: O are obviously enhanced when the GO was grafted with amino acids, indicating the reduction of GO, which is also proved in SI Figure S5. So, the reduction of O did make contribution in reducing the work function of GO during the process of functionalized with amino acids. However, the results did not exhibit any positive relationship between the change in the work function and the extent of reduction. For example, GO−Cys and GO−Asp

possess the same C: O ratio (6.1: 1) but different work function. As mentioned before, Cys is a type of amino acid with electron−rich thiol group, so it changes more work function reduction than Asp when it grafted on GO. Moreover, the work functions of GO−AA were all lower than that of the original graphite, which was measured to be about 4.7 eV. Therefore, we can deduce that the reduction of O makes far less contribution than amino acid molecular in decreasing the work function of GO. In contrast, the O reduction of GO is favored to the enhancement of conductivity so that it is suitable for use as electrodes.

PEDOT: PSS is a type of conductive polymer with some unique advantages such as water-solubility, ease of deposition process, high conductivity, and high transparency[29, 30]. In order to easily and conveniently form a uniform high conductivity film by solution process, GO or graphene are usually composited with the conductive polymer PEDOT: PSS for use as transparent electrodes[31, 32]. We also investigated the work function of the compounds of GO−AA with PEDOT: PSS. Figure 3b compares the UPS spectra of pure PEDOT: PSS, compounds of PEDOT: PSS with GO, and compounds of PEDOT: PSS with GO functionalized with amino acids Phe, Ala, Asp, or Glu. The original work function of pure PEDOT: PSS is about 4.7 eV; however, that of the PEDOT: PSS blended with GO increases to about 5.0 eV. The work function of compounds with GO−AA decreases to less than 4.5 eV. The results show that the composite films have also a large range of work function, from 4.0 to 5.0 eV, to select for matching with the energy level of semiconductors.

Figure 4a shows the SEM images of films fabricated with the blend of PEDOT:

PSS and GO–Cys. PEDOT: PSS is distributed uniformly on the surface of GO–Cys. Figure 4b shows the TEM images of GO–Cys/PEDOT: PSS composites, exhibiting that the GO–Cys sheet is tightly covered by the PEODT: PSS, leading to the formation of a contiguous film. To disclose the electrical properties and transparency of the films of GO−AA/PEDOT: PSS composites, the conductivity and transparency of the films were measured and the results are shown in Figure 5. Different amounts of GO–Cys were added to PEDOT: PSS and then the composite was spin coated on glass at 1500 r min^{-1} for 15 s. The thickness of films was about 20 nm. The conductivity of PEDOT: PSS film was 1667 S cm^{-1}. After adding 3 wt.% of graphene compounds, the conductivity of films was the highest at 1749 S cm^{-1}. When the weight percentage of GO–Cys was more than 3%, the conductivity of films decreased. This might be due to the stacking of GO–Cys. The conductivity of ITO was also measured for comparisons. ITO with shunt resistance of 6 and 15 Ω sq^{-1} has corresponding conductivity of 7.0 x 10^3 and 2.8 x 10^3 S cm^{-1}, which is the near level to the conductivity of the composite film of PEDOT: PSS/GO–Cys. The transmittance of GO−Cys/PEDOT: PSS films was up to 90% at 300–900 nm, which reaches the requirement for various ultraviolet to near−infrared optoelectronic devices.

To prove the application of GO−AA in photoelectric devices, organic photodetectors (OPDs) were fabricated using ITO/GO–Cys or ITO/GO–Cys+PEDOT: PSS as the cathode. OPD with pure ITO was also fabricated for comparisons. The performance of the photodetectors is shown in Figure 6. Figure 6a shows that the device with ITO/GO–Cys has approximately an order of magnitude reduction of the

dark current density under the voltage ranging from −2 to 0 V. In particular, the device with the compound GO–Cys+PEDOT: PSS displays a remarkably low dark current density of 4.4×10^{-10} A cm^{-2} at 0 V. Moreover, the OPDs with GO or its compound with PEDPT: PSS possess high photoresponsivity. The photocurrent responsivity (RI) of the devices is displayed in Figure 6b, indicating that OPDs with GO–Cys or GO–Cys+PEDOT has higher RI at a wide range of wavelength from 350 to 780 nm compared to the device without GO–Cys. The combined results of low dark current and high photoresponsivity lead to high normalized detectivity (D*) which is also shown in Figure 6b. The highest D* of the device with the blend of GO–Cys with PEDOT: PSS is up to 5.7×10^{12} Jones at the wavelength of 620 nm. The D* is close to the highest level of the organic photodetectors with a diode structure according to the recent reports[33, 34].

Figure 6c shows the time−resolved photo response voltages (Vrp) of the devices. The devices were illuminated under a green laser source driven by a rectangular wave voltage. With ON or OFF for the light irradiation switch, the blank device showed an increase time of 35.9 μs and a decay time of 174.4 μs. However, the device with ITO/GO–Cys as cathode showed a rise time of 27.8 μs and a decay time of 130.2 μs. The device with GO–Cys+PEDOT: PSS exhibited fast response compared to the above mentioned two devices, with a rise time of 13.2 μs and decay time of 98.7 μs. The −3 dB bandwidth shown in Figure 6d, increases from 10.3 kHz for the blank device to 30.1 kHz for the device with ITO/GO−Cys+PEDOT: PSS.

Conclusions

In summary, we reported that the work function of GO can be controlled through a wide range by chemically grafting amino acids on GO. The work function of GO−AA can be significantly reduced from 5.3 down to 4.0 eV, which is even lower than that of original graphite. In addition, by mixing the conductive polymer PEDOT: PSS with the novel GO−AA, the work function of the compound films can be tuned from 4.0 to 5.0 eV and the films have high UV−Visible transmittance and conductivity with the level comparable with the commonly used transparent conductive electrode of ITO. The OPDs fabricated with the cathodes containing GO−Cys or PEDOT: PSS+GO−Cys have a highest D* of 5.7×10^{12} Jones at −0.1 V complying with a fast response speed. The results in this work imply that these functionalized GOs have a promising potential to act as transparent electrode materials in the application of organic, inorganic, and hybrid electronic devices.

Experimental Section

Preparation of graphene oxide. Graphene oxide was synthesized by consulting a modified Hummers method[5]. Concentrated sulfuric acid (25 mL) was added to a mixture of graphite (1.0 g) and sodium nitrate (0.6 g) at room temperature. Potassium permanganate (3.7 g) was added slowly in portions to keep the reaction temperature below 5 °C. Sulfuric acid was inserted into the graphite layers at this stage. The reaction temperature of the mixture was kept at 35 °C with the stirring for 2 h, and then was increased to 60 ^{o}C for stewing mixture for 6 h. Then, 45 mL water was

slowly poured into the solution under vigorous stirring, and dark brown suspension was produced. The suspension was treated further by adding the mixture of aqueous hydrogen peroxide (3.5 mL, 34.5%) and water (22.5 mL) to convert the residual permanganate and manganese dioxide into soluble manganese sulfate. Graphene oxides were separated from the reaction mixture by filtration. The powder of graphene oxides was washed for 3 times with diluted hydrochloric acid (1.0 mol L^{-1}, 25 mL). Ultrasonic treatment was carried out for 10 minutes before washing. The obtained product was dried for 24 h under vacuum, and then grinded and dispersed into distilled water. Finally, the product was ultrasonically treated for 3 h under 200 W.

Preparation of Amino−Acid−Functionalized Graphene Hybrids. Firstly, GO (200 mg) was ultrasonically treated with 10 g NaOH and 10 g $ClCH_2COONa$ for 4 h. Carboxylated graphene oxide sheets were separated from the reaction mixture by filtration, and washed by HCl. The product was dried at 50°C for 24 h, and then treated with $SOCl_2$ (80 mL) at 65°C for 24 h. After the completion of the reaction, the redundant $SOCl_2$ was evaporated, and the product was washed by anhydrous tetrahydrofuran (THF). Then, the product was reacted with excess amino acids at 90 °C for 24 h in the presence of anhydrous DMF (40 mL). To remove the unreacted amino acids, the product was washed by Na_2CO_3, ethanol and deionized water in turn for twice. Finally, the product was dried under vacuum at 50 °C. Graphene oxide functionalized by different amino acids materials were denoted as GO−AA (AA denotes as amino acids).

Device Fabrication. ITO were ultrasonically cleaned with acetone, detergent,

deionised water, and isopropyl alcohol and then treated by UV-ozone for 15 min. GO−Cys (2 mg ml^{-1}) or GO−Cys (2 mg ml^{-1})+PEDOT: PSS (15 mg ml^{-1}) was spin-coated on ITO at speed of 500 rpm for 18 s for twice. Afterwards, a solution of 17 mg ml^{-1} P3HT and 17 mg ml^{-1} PCBM in dichlorobenzene was spin-coated at a slow speed of 400 rpm for 8 s. Then, they were annealed at 110 ^{o}C for over 1 h. Finally, 10 nm thick MoO_3 and 120 nm thick Al was deposited on top of the active layer as anode. The typical active area of the devices was about 0.12 cm^2.

Materials characterization. The products were characterized by scanning electron microscopy (SEM, HITACHI S−4700), X−Ray diffraction (XRD, Rigaku D/Max 2500 PC). X−ray and ultraviolet photoelectron spectroscopy (XPS and UPS, Kratos AXIS Ultra−DLD), transmission electron microscopy (TEM, JEM−2100HR), atomic force microscope (AFM, Brucker icon), Fourier transform infrared spectroscopy (FT−IR, Nicolet 6700). For the XPS and UPS measurements, Au deposited on Si wafer was used as substrates, and the GO, GO−AA and PEDOT: PSS compounds were spin coated on top of the substrates.

Characterization of GO-AA/PEDOT: PSS composite films. 0，1 wt.%，3 wt.% and 5 wt.% GO−Cys were added to the solution of PEDOT: PSS (15 mg mL^{-1}), respectively, and then the composites were under ultrasonic treatment for 1 hour. GO−AA/PEDOT: PSS composite films were fabricated via spin-coating at 1500 rpm for 5 s, and annealed at 120 ^{o}C for 1 h. The film thickness is about 20 nm. Finally, the conductivity was measured by Four−point probes and the transmittance was measured by ultraviolet−visible spectrophotometer.

Device Characterization. The dark current was measured by Keithey 4200 source meter unit with devices in a shielding box. The responsivity was measured with a quantum efficiency (QE)/IPCE measurement system (SR830, Stanford Research Systems). Reverse bias on the devices was provided by a constant output voltage from a 20 MHz Function/Arbitrary Waveform Generator (33220A, Agilent). To measure the transient response, a laser diode was powered by a square pulse from the Waveform Generator (33220A, Agilent). Photocurrent of the devices was measured by a 100 MHz digital oscilloscope (TDS 1012C−SC, Tektronix). Considering the dark current is the main source of noise current, the normalized detectivity (D*) can be calculated by $D^* = \frac{R_I}{\sqrt{2qJ_d}}$, where RI is the photocurrent responsivity, Jd is the density of dark current, and q is the electron charge with value of 1.6×10^{-19} Coulombs.

Acknowledgements

This work is supported by the Shenzhen Research Foundation Project (Grants JCYJ20140417161, and KQCX20140521144147315).

References

1. G. Eda, Y. Y. Lin, S. Miller, C. W. Chen, W. F. Su, M. Chhowalla, *Appl. Phys. Lett.* **2008**, 92, 1441-1446.
2. X. Wang, L. Zhi, K. Müllen, *Nano Lett.* **2008**, 8, 323-327.
3. J. Wu, M. Agrawal, H. A. Becerril, Z. Bao, Z. Liu, Y. Chen, P. Peumans, *ACS*

Nano. **2009**, 4, 43-48.

4. Q. Su, S. Pang, V. Alijani, C. Li, X. Feng, K. Müllen, *Adv. Mater.* **2009**, 21, 3191-3195.
5. W. Hummers, R. Offeman, *J. Am. Chem. Soc.* **1958**, 80, 1339.
6. S. Stankovich, D. A. Dikin, R. D. Piner, K. A. Kohlhaas, A. Kleinhammes, Y. Y. Jia, Y. Wu, S. T. Nguyen, R. S. Ruoff, *Carbon.* **2007**, 45, 1558–1565.
7. O. O. Kapitanova, G. N. Panin, A. N. Baranov, *J. Kor. Phys. Soc.* **2012**, 60, 1789-1793.
8. G. Eda, G. Fanchini, M. Chhowalla, *Nat. Nanotechnol.* **2008**, 3, 270-274.
9. Z. Yin, S. Sun, T. Salim, S. X. Wu, X. Huang, Q. Y. He, Y. M. Lam, H. Zhang, *ACS Nano.* **2010**, 4, 5263-5268.
10. L. G. D. Arco, Y. Zhang, C. W. Schlenker, K. Ryu, M. E. Thompson, C. Zhou, *ACS Nano.* **2010**, 4, 2865–2873.
11. Y. Wang, X. Chen, Y. Zhong, F. Zhu, K. P. Loh, *Appl. Phys. Lett.* **2009**, 95, 063302.
12. Q. Lu, Y. Y. Feng, X. Q. Zhang, Y. Li, W. Feng, *Tech. Sci.* **2010**, 9, 2311-2319.
13. J. Wu, H. A. Becerril, Bao, Z.; Z. Liu, Y. Chen, P. Peumans, *Appl. Phys. Lett.* **2008**, 92, 263302.
14. Y. Xu, G. Long, L. Huang, Y. Huang, X. Wan, Y. Ma, Y. Chen, *Carbon*. **2010**, 48, 3308–3311.
15. L. M. Zhang, J. G. Xia, Q. H. Zhao, L. W. Liu, Z. J. Zhang, *Small*. **2010**, 6, 537-44.

16. H. Bao, Y. Pan, Y. Ping, Y. Ping, N. G. Sahoo, T. Wu, L. Li, J. Li, L. H. Gan, *Small*. **2011**, 7, 1569-1578.

17. Q. Li, F. Fei, W. Yang, W. Feng, P. J. Ji, *Ind. Eng. Chem. Res.* **2013**, 52, 6343-6348.

18. W. F. Zhang, S. S. Wang, J. J. Ji, Y. Li, G. L. Zhang, F. B. Zhang, X. B. Fan, *Nanoscale*. **2013**, 5, 6030-6033.

19. R. Devi, G. Prabhavathi, R. Yamuna, S. Ramakrishnan, N. K. Kothurkar, *J. Chem. Sci.* **2014**, 126, 75-83.

20. S. T. Sun, Y. W. Cao, J. C. Feng, P. Y. Wu, *J. Mater. Chem.* **2010**, 20, 5605-5607.

21. J. H. Zhu, Y. X. Li, Y. Chen, J. Wang, B. Zhang, J. J. Zhang, W. J. Blau, *Carbon.* **2011**, 49, 1900–1905.

22. D. Depan, T. C. Pesacreta, R. D. K. Misra, *Bio. Sci.* **2014**, 2, 264-274.

23. Y. Si, E. T. Samulski, *Nano Lett.* **2008**, 8, 1679-1682.

24. F. Lu, S. H. Zhang, H. J. Gao, J. Han, L. Q. Zheng, *ACS Appl. Mater. Inter.* **2012**, 4, 3278-3284.

25. T. Xu, Q. Qiao, *Energy Environ. Sci.* **2011**, 8, 2700-2720.

26. X. Y. Deng, R. M. Nie, A. Y. Li, H. X. Wei, S. Z. Zheng, W. B. Huang, Y. Q. Mo, Y. R. Su, Q. K. Wang, Y. Q. Li, J. X. Tang, J. B. Xu, K.-Y. Wong, *Adv. Mater. Inter.* **2014**, 1, 1400215.

27. A. Y. Li, R. M. Nie, X. Y. Deng, H. X. Wei, S. Z. Zheng, Y. Q. Li, J. X. Tang, K. Y. Wong, *Appl. Phys. Lett.* **2014**, 104, 123303.

28. R. M. Nie, A. Y. Li, X. Y. Deng, *J. Mater. Chem. A.* **2014**, 19, 6734-6739.

29. D. Yoo, J. Kim, J. H. Kim, **2014**, 7, 717-730.

30. H. Yan, T. Jo, H. Okuzaki, *J. Polymer.* **2009**, 41, 1028–1029.

31. W. Li, W. Bi, S. Wang, *J. Mater. Sci.* **2015**, 50, 2148-2157.

32. Y. F. Liu,; J. Feng, Y. F. Zhang, H. F. Cui, D. Yin, Y. G. Bi, J. F. Song, Q. D. Chen H. B. Sun, *Org. Electron*. **2015**, 26, 81–85.

33. X. Gong, M. H. Tong, Y. J. Xia, W. Z. Cai, J. S. Moon, Y. Cao, G. Yu, C. H. Shieh, B. Nilsson, A. J. Heeger, *Science*, **2009**, 325, 1665-7.

34. R. M. Nie, Y. Y. Wang, X. Y. Deng, *ACS Appl. Mater. Inter*, **2014**, 6, 7032-703.

Graphical Table of Contents:

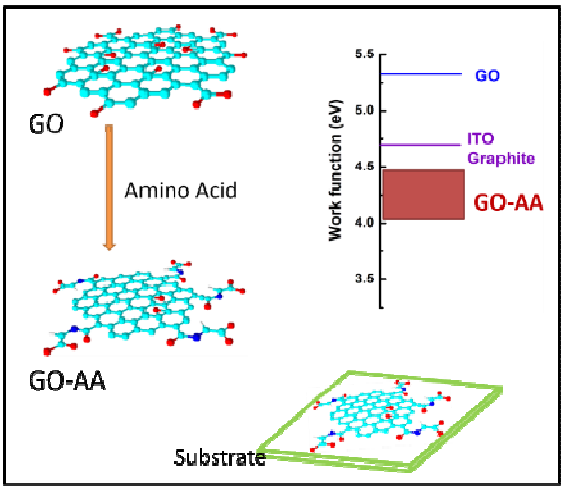

Table 1. C: O ratio and work function of graphene oxide functionalized by different amino acids.

GO−AA	GO−Cys	GO−Ala	GO−Phe	GO−Asp	GO−Lys	GO−Arg	GO
C:O ratio	6.0 : 1	3.4 : 1	2.6 : 1	6.0 : 1	2.5 : 1	3.2 : 1	1.4 : 1
Work function (eV)	4.00	4.18	4.22	4.30	4.45	4.50	5.30

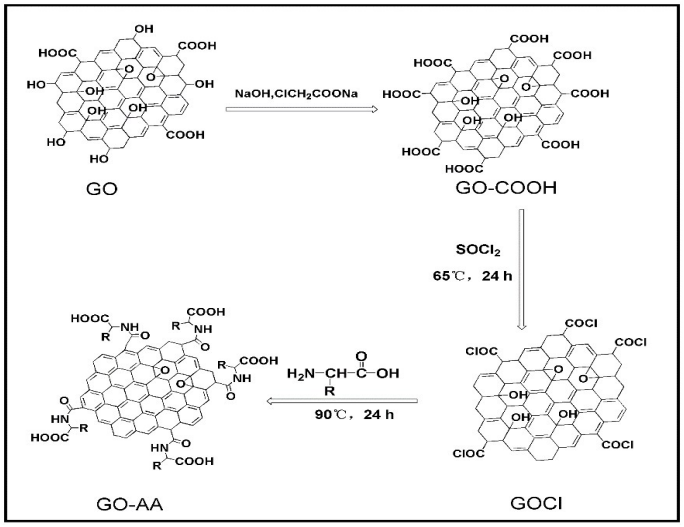

Scheme 1. Synthesis of graphene oxide functionalized by amino acids

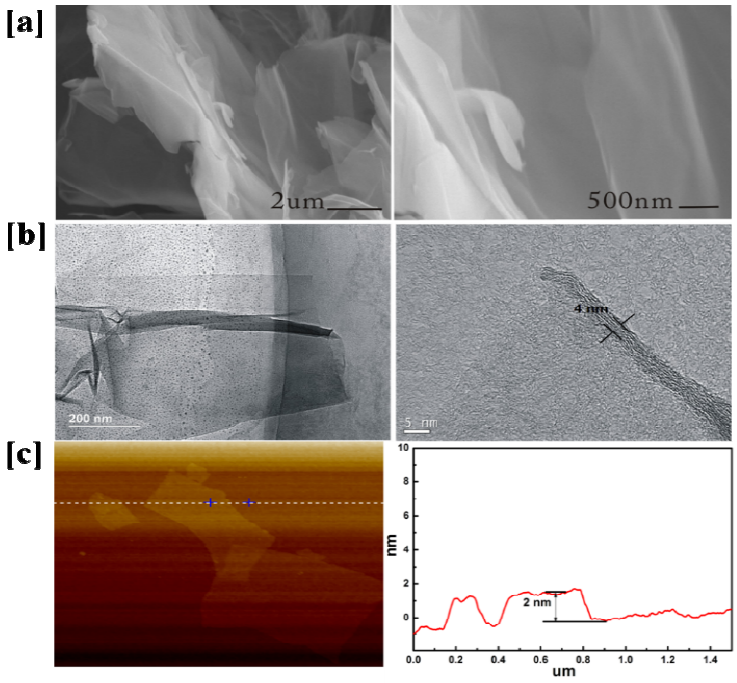

Figure 1. SEM images (a), TEM images (b), AFM image and section profiles (c) of graphene oxide functionalized by cysteine.

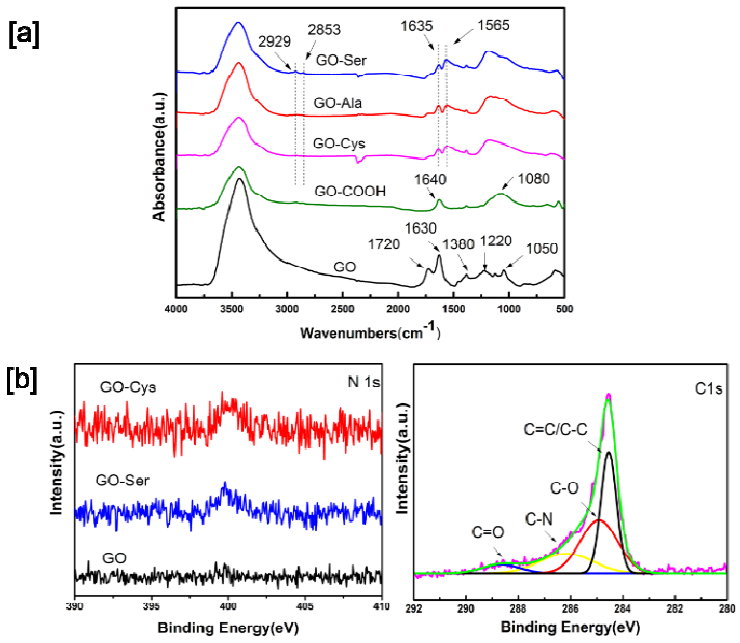

Figure 2. FT−IR spectra of GO−AA compounds (a), and XPS N1s spectra for GO, GO−Cys, GO−Ser and C 1s spectrum for GO−Cys (b)

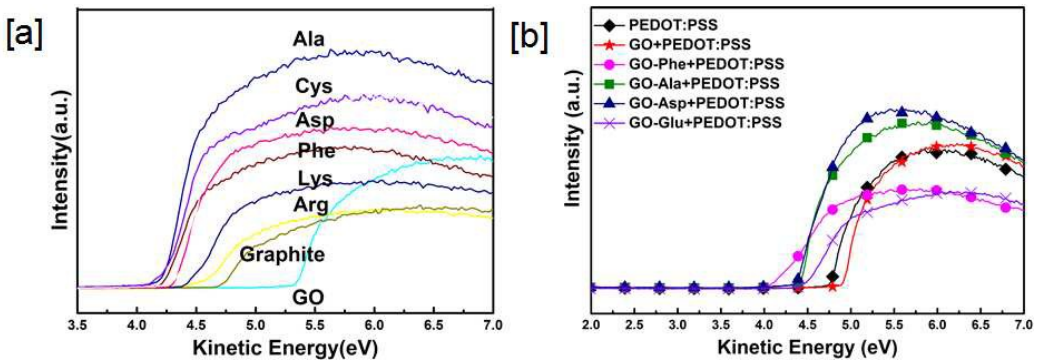

Figure 3. UPS spectra of GO, GO functionalized with amino acids (a) and composite Films of PEDOT: PSS with GO or GO functionalized with amino acids (b).

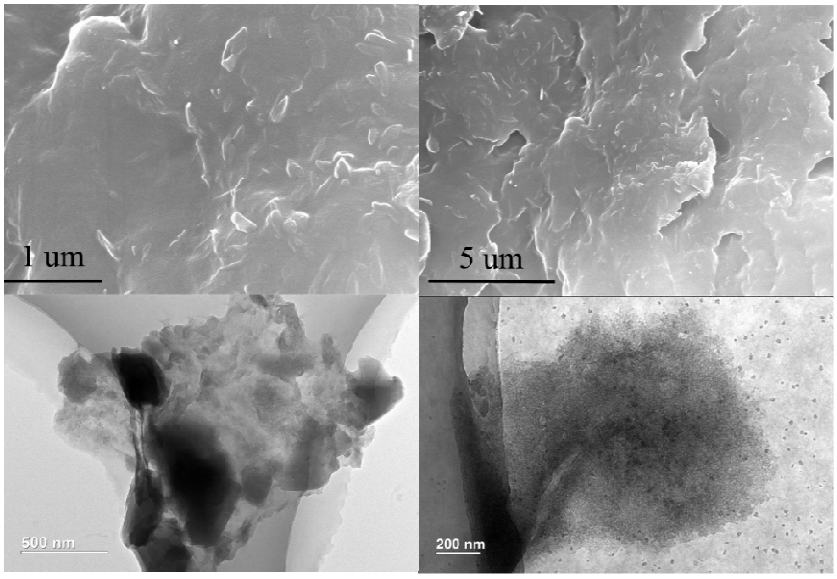

Figure 4. SEM images (a) films fabricated with the blend of PEDOT: PSS and GO−Cys. TEM images (b) of GO−Cys/PEDOT: PSS composites.

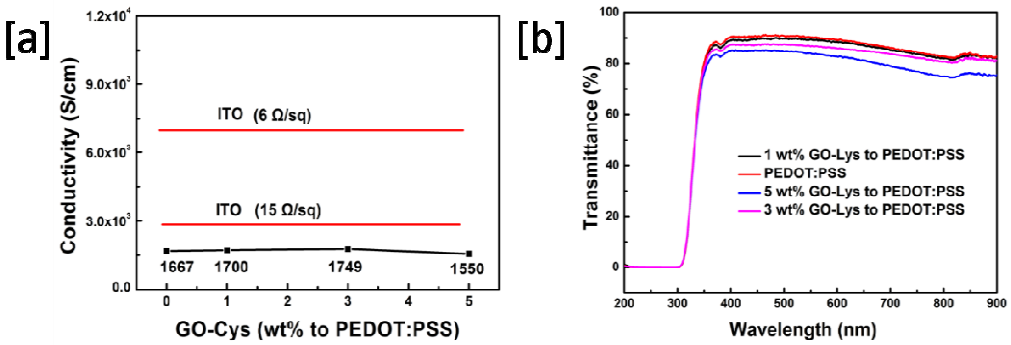

Figure 5. The conductivity (a) and transmittance (b) of films fabricated with different mount of GO−Cys and PEDOT: PSS composites.

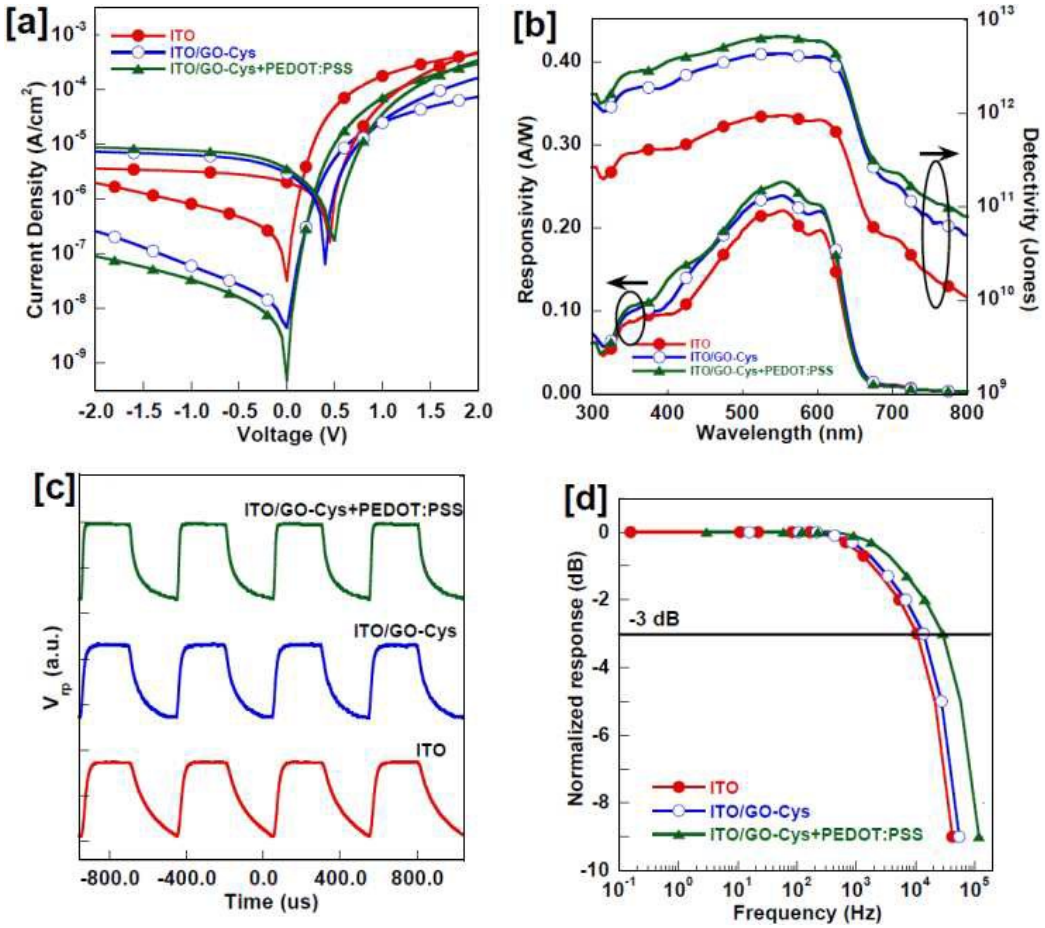

Figure 6. (a) Current−density to voltage (J−V) characteristics of OPDs with ITO, ITO/GO−Cys or ITO/GO−Cys+PEDOT: PSS as the cathode. (b) Responsivity and detectivity under −0.1 V versus the wavelength of the OPDs. (c) Transient response under short−circuit conditions of OPDs. (d) Frequency response of OPDs.